

DYNAMICS OF A THICK-WALLED SPHERICAL CASING LOADED WITH A TIME DEPENDING INTERNAL PRESSURE

EDWARD WŁODARCZYK

*Military University of Technology, Faculty of Mechatronics, Warsaw, Poland
e-mail: edward.wlodarczyk@wat.edu.pl*

MARIUSZ ZIELENKIEWICZ

*Military Institute of Armament Technology, Zielonka, Poland
e-mail: m.zielenkiewicz@chello.pl*

The problem of radial vibration of a thick-walled spherical casing, loaded with an internal pressure, which is a time function, is studied. We assumed that the material of the casing is incompressible. Furthermore, the linear elasticity theory is applied in the considerations. By means of these simplifications, an analytical solution of dynamics of the thick-walled spherical casing loaded with the internal pressure has been obtained. This solution may be used for estimation of strength of spherical ballistic casings which are applied to explosive driven specimen in ring tests. Moreover, the results of this paper contribute to the theory of vibration of continuous engineering systems.

Key words: dynamics, thick-walled spherical casing, forced vibrations, internal surge-pressure, incompressible material

1. Introduction

One of experimental methods on investigating mechanical properties of dynamically loaded materials is the ring test method (Włodarczyk and Janiszewski, 2004; Włodarczyk *et al.*, 2005b). In this method, a thin-walled ring made of the tested material is driven by detonation products of High Explosive (HE) or by a high energy impulse of an electromagnetic field, and the radial displacement of the ring or velocity of its expansion is recorded.

Thick-walled metal casings of cylindrical or spherical symmetry are used to eliminate the influence of perturbations caused by HE detonation products. The thin-walled ring is placed on the external surface of the casing that is fully or partially filled with HE. After detonation, the compression shock wave propagates in the casing wall, which reflecting from the ring contact surface, drives it up to high velocity. Reaction of high explosive detonation products with various geometry casings takes place also in artillery shells, grenades and bombs as well as in barrels of projectiling systems (Walters and Zukas, 1989; Włodarczyk *et al.*, 2004). These problems are the subject of various theoretical and experimental researches.

Radial vibrations of a thick-walled pipe forced by internal surge-pressure uniformly distributed along its length, was studied in Włodarczyk *et al.* (2005a). The material of the pipe was approximated by an incompressible linearly-elastic medium. For this kind of material, a closed-form analytical solution to the problem of dynamics was obtained. It was found that the pipe made of an incompressible material, loaded by an internal pressure, responds like a system with one degree of freedom. For example, a pipe loaded with a rapidly applied and constant internal pressure vibrates with a constant angular frequency ω_0 around the state determined through the static solution to Lamé's problem.

In this paper, an analogous problem of a thick-walled spherical casing has been considered. The comparison of analytical results determining dynamical states of both kinds of objects has significant practical meaning and is an additional contribution of knowledge to the theory of vibrations of continuous media.

2. Formulation of the problem

Dynamic states of the radial displacement and of the stress as well as strain in a spherical casing loaded by an internal pressure $p(t)$ have been determined.

Let a and b denote the internal and external radii of the casing. The problem has been solved in the spherical system of Lagrangian coordinates r, ϕ, θ . Taking into account spherical symmetry, the problem can be assumed as a spatially one-dimensional boundary value problem. Therefore, the states of stress and strain in the material of the casing can be represented by the following components:

$$\begin{aligned} \sigma_r & \quad - \quad \text{radial stress} \\ \sigma_\varphi = \sigma_\theta & \quad - \quad \text{tangential stresses} \end{aligned}$$

ε_r – radial strain
 $\varepsilon_\varphi = \varepsilon_\theta$ – tangential strains.

The rest of components of the stress and strain tensors equal to zero in this coordinate system.

The problem has been solved according to the linear elasticity theory. Therefore, the following relations can be written (Nowacki, 1970)

$$\varepsilon_r(r, t) = \frac{\partial u(r, t)}{\partial r} \quad \varepsilon_\varphi(r, t) = \varepsilon_\theta(r, t) = \frac{u(r, t)}{r} \quad (2.1)$$

$$\sigma_r(r, t) - \sigma_\varphi(r, t) = 2\mu(\varepsilon_r - \varepsilon_\varphi)$$

where u and r denote the radial displacement of an infinitesimal element of the casing and its Lagrangian coordinate, while μ denote Lamé's constant

$$\mu = \frac{E}{2(1 + \nu)} \quad (2.2)$$

The symbols E and ν denote Young's modulus and Poisson's ratio.

Using the Lagrangian coordinate r for the infinitesimal element and taking into account the spherical symmetry and the mass conservation law, it can be written

$$(r + u)^2 \left(1 + \frac{\partial u}{\partial r}\right) = \frac{\rho_0}{\rho} r^2 \quad (2.3)$$

where symbols ρ_0 and ρ denote the initial and current density of the material of the casing.

For metals exposed to pressures of the order of a few thousands MPa, it can be assumed that $\rho \approx \rho_0 = \text{const}$. This simplification has been discussed in Włodarczyk and Janiszewski (2004). The error caused by this is less than a few percents. Taking into account this assumption, for small strains

$$\varepsilon_\varphi \varepsilon_r = \frac{u}{r} \frac{\partial u}{\partial r} \approx 0 \quad \varepsilon_\varphi^2 = \left(\frac{u}{r}\right)^2 \approx 0$$

equation (2.3) can be reduced to the following form

$$\frac{\partial u}{\partial r} + 2\frac{u}{r} = 0 \quad (2.4)$$

Using the Lagrangian coordinate r to formulate the condition of dynamic equilibrium, the equation of motion of the infinitesimal element, after transformation, can be written as

$$\rho_0 \frac{\partial^2 u}{\partial t^2} = \left(1 + \frac{u}{r}\right)^2 \frac{\partial \sigma_r}{\partial r} + 2\left(1 + \frac{u}{r}\right) \left(1 + \frac{\partial u}{\partial r}\right) \frac{\sigma_r - \sigma_\varphi}{r} \quad (2.5)$$

For small strains, and neglecting small quantities of higher orders, equation (2.5) can be reduced to the following form

$$\frac{\partial \sigma_r}{\partial r} + 2 \frac{\sigma_r - \sigma_\varphi}{r} = \rho_0 \frac{\partial^2 u}{\partial t^2} \quad (2.6)$$

The linearized system of equations (2.4) and (2.6) has been solved for the following boundary conditions

$$\begin{aligned} \sigma_r(a, t) &= -p(t) & \text{for } r &= a \\ \sigma_r(b, t) &\equiv 0 & \text{for } r &= b \\ u(r, 0) &= 0 & \text{and } v(r, 0) &= \left. \frac{\partial u}{\partial t} \right|_{t=0} = 0 \end{aligned} \quad (2.7)$$

The structure of the analytical solution to the above formulated problem has been presented below.

3. Analytical solution to the problem

The general solution of equation (2.4) has the following form

$$u(r, t) = \frac{C(t)}{r^2} \quad (3.1)$$

where $C(t)$ denotes a continuous and twice differentiable time function.

From expressions (2.1) and (3.1), we have

$$\varepsilon_r(r, t) = -2 \frac{C(t)}{r^3} \quad \varepsilon_\varphi(r, t) = \varepsilon_\theta(r, t) = \frac{C(t)}{r^3} \quad (3.2)$$

$$\sigma_r(r, t) - \sigma_\varphi(r, t) = -6\mu \frac{C(t)}{r^3}$$

Upon substitution of expressions (3.1) and (3.2)₃ into equation of motion (2.6) and integration in respect to r , the following expression has been obtained

$$\sigma_r(r, t) = -4\mu \frac{C(t)}{r^3} - \rho_0 \frac{\ddot{C}(t)}{r} + A(t) \quad (3.3)$$

where $\ddot{C}(t) = d^2C(t)/dt^2$, and $A(t)$ denotes an arbitrary time function. From boundary condition (2.7)₂ and solution (3.3), we obtain

$$A(t) = 4\mu \frac{C(t)}{b^3} + \rho_0 \frac{\ddot{C}(t)}{b} \quad (3.4)$$

Finally, after substitution of expression (3.4) into equation (3.3) and simple transformations, the radial stress $\sigma_r(r, t)$ can be expressed by the following formula

$$\sigma_r(r, t) = \rho_0 \frac{r-b}{br} \ddot{C}(t) + 4\mu \frac{r^3 - b^3}{b^3 r^3} C(t) \quad (3.5)$$

In turn, after substitution of expression (3.5) into boundary condition (2.7)₁ and transformation, we have

$$\ddot{C}(t) + 4 \frac{\mu}{\rho_0} \frac{b^2 + ab + a^2}{a^2 b^2} C(t) = \frac{ab}{\rho_0(b-a)} p(t) \quad (3.6)$$

Let us introduce the following symbols

$$c = \sqrt{\frac{\mu}{\rho_0}} \quad \beta = \frac{b}{a} \quad (3.7)$$

$$\omega_0^2 = 4 \frac{\mu}{\rho_0} \frac{b^2 + ab + a^2}{a^2 b^2} = 4 \left(\frac{c}{a}\right)^2 \frac{\beta^2 + \beta + 1}{\beta^2}$$

where c denotes the propagation velocity of a transverse wave in the material of the casing, and ω_0 is the angular frequency of its free vibrations. It has been found that, similarly to the incompressible pipe (Włodarczyk *et al.*, 2005a), the thick-walled spherical casing has only one angular frequency (pulsatance) and responds like a system with one degree of freedom.

Taking into account expressions (3.7) and (2.7)₃, the function $C(t)$ can be determined by the following equation

$$\ddot{C}(t) + \omega_0^2 C(t) = \frac{a}{\rho_0} \frac{\beta}{\beta - 1} p(t) \quad (3.8)$$

with the homogeneous initial conditions

$$C(0) = 0 \quad \dot{C}(t) = \frac{dC(t)}{dt} \Big|_{t=0} = 0 \quad (3.9)$$

The solution to equation (3.8) with initial conditions (3.9) has the following form

$$C(t) = \frac{a}{\rho_0 \omega_0} \frac{\beta}{\beta - 1} \int_0^t p(\tau) \sin[\omega_0(t - \tau)] d\tau \quad (3.10)$$

In turn, from equation (3.8), we obtain

$$\ddot{C}(t) = \frac{a}{\rho_0} \frac{\beta}{\beta - 1} p(t) - \omega_0^2 C(t) \quad (3.11)$$

As it can be seen, the function $C(t)$ is determined by means of formula (3.10). In turn, the function $C(t)$ fully determines all unknown quantities of the problem, namely

$$\begin{aligned}
 u(r, t) &= \frac{C(t)}{r^2} \\
 v(r, t) &= \frac{\partial u}{\partial t} = \frac{\dot{C}(t)}{r^2} & \dot{C}(t) &= \frac{dC(t)}{dt} \\
 \varepsilon_r(r, t) &= \frac{\partial u}{\partial r} = -2 \frac{C(t)}{r^3} & \varepsilon_\varphi(r, t) = \varepsilon_\theta(r, t) &= \frac{u}{r} = \frac{C(t)}{r^3} \\
 \sigma_r(r, t) &= \frac{1}{\beta - 1} \left(1 - \frac{b}{r}\right) p(t) + 4 \frac{\mu}{b^3} \left[1 - \left(\frac{b}{r}\right)^3 - \frac{b^2 + ab + a^2}{a^2} \left(1 - \frac{b}{r}\right)\right] C(t) \\
 \sigma_\varphi(r, t) &= \frac{1}{\beta - 1} \left(1 - \frac{b}{r}\right) p(t) + 2 \frac{\mu}{b^3} \left[2 + \left(\frac{b}{r}\right)^3 - 2 \frac{b^2 + ab + a^2}{a^2} \left(1 - \frac{b}{r}\right)\right] C(t)
 \end{aligned} \tag{3.12}$$

If the pressure inside of the casing is generated statically, i.e.: $p(t) = p_s = \text{const}$, then $C(t) = C_s = \text{const}$, $\dot{C}(t) = 0$, and taking into account expression (3.5), we have

$$\sigma_r(r, t) = \sigma_{rs}(r) = -4 \frac{\mu}{b^3} \frac{b^3 - r^3}{b^3 + r^3} C_s \tag{3.13}$$

Subsequently, from the boundary condition $\sigma_{rs}(a) = -p_s$ and expression (3.13), we obtain

$$C_s = \frac{1}{4} \frac{p_s}{\mu} \frac{a^3 b^3}{b^3 - a^3} = \frac{1}{4} \frac{p_s}{\mu} \frac{\beta^3}{\beta^3 - 1} a^3 \tag{3.14}$$

Through replacing the function $C(t)$ with the symbol C_s in expressions (3.12)_{1,3-5}, the unknown quantities of the problem can be determined for the static load.

4. Dynamic state of parameters of the spherical casing loaded with an internal surge pressure $p = \text{const}$

In order to simplify quantitative analysis of the particular parameters: displacement, velocity, strains and stresses, the following dimensionless quantities have been introduced

$$\begin{aligned}
\xi &= \frac{r}{a} & \eta &= \frac{t}{T_0} & \beta &= \frac{b}{a} & U &= \frac{u}{a} \\
V &= \frac{v}{c} & \bar{C} &= \frac{C}{a^3} & F &= \frac{\mu}{p} & S_r &= \frac{\sigma_r}{p} \\
S_\varphi &= \frac{\sigma_\varphi}{p} & U_s &= \frac{u_s}{a} & \bar{C}_s &= \frac{C_s}{a^3} & S_{rs} &= \frac{\sigma_{rs}}{p_s} \\
S_{\varphi s} &= \frac{\sigma_{\varphi s}}{p_s} & \bar{\omega}_0 &= \frac{\omega_0}{(c/a)}
\end{aligned} \tag{4.1}$$

where T_0 denotes the natural vibration period of the casing

$$T_0 = \frac{2\pi}{\omega_0} \tag{4.2}$$

After substitution $p(\tau) = p = \text{const}$ into expression (3.10), integration within the range $0 - t$ and taking into account dimensionless quantities (4.1), we obtain

$$\bar{C}(t) = \frac{1}{4F} \frac{\beta^3}{\beta^3 - 1} (1 - \cos 2\pi\eta) = \bar{C}_s (1 - \cos 2\pi\eta) \tag{4.3}$$

$$\bar{C}_s = \frac{1}{4F} \frac{\beta^3}{\beta^3 - 1}$$

The remaining quantities determining the mechanical state of the casing, according to expressions (3.12), (3.13) and (4.3), can be written as follows:

— for the dynamic load

$$U(\xi, \eta) = \frac{\bar{C}_s}{\xi^2} (1 - \cos 2\pi\eta) \tag{4.4}$$

$$V(\xi, \eta) = \frac{1}{2F} \frac{\beta^2 \sqrt{\beta^2 + \beta + 1}}{\beta^3 - 1} \frac{1}{\xi^2} \sin 2\pi\eta \tag{4.5}$$

$$\varepsilon_\varphi(\xi, \eta) = -\frac{1}{2} \varepsilon_r(\xi, \eta) = \frac{\bar{C}_s}{\xi^3} (1 - \cos 2\pi\eta) \tag{4.6}$$

$$S_r(\xi, \eta) = -\frac{1}{\beta^3 - 1} \left[\left(\frac{\beta}{\xi} \right)^3 - 1 \right] + A_r(\xi) \cos 2\pi\eta \tag{4.7}$$

$$A_r(\xi) = \frac{1}{\beta^3 - 1} \left[\left(\frac{\beta}{\xi} \right)^3 - (\beta^2 + \beta + 1) \left(\frac{\beta}{\xi} - 1 \right) - 1 \right] \tag{4.8}$$

$$S_\varphi(\xi, \eta) = \frac{1}{2(\beta^3 - 1)} \left[2 + \left(\frac{\beta}{\xi} \right)^3 \right] - A_\varphi(\xi) \cos 2\pi\eta \tag{4.9}$$

$$A_\varphi(\xi) = \frac{1}{2(\beta^3 - 1)} \left[\left(\frac{\beta}{\xi} \right)^3 + 2(\beta^2 + \beta + 1) \left(\frac{\beta}{\xi} - 1 \right) + 2 \right] \tag{4.10}$$

$$\bar{\omega}_0 = 2 \frac{\sqrt{\beta^2 + \beta + 1}}{\beta} \quad (4.11)$$

— for the static load

$$U_s(\xi) = \frac{1}{4F} \frac{\beta^3}{\beta^3 - 1} \frac{1}{\xi^2} = \frac{\bar{C}_s}{\xi^2} \quad (4.12)$$

$$\varepsilon_{\varphi s}(\xi) = -\frac{1}{2} \varepsilon_{rs}(\xi) = \frac{\bar{C}_s}{\xi^3} \quad (4.13)$$

$$S_{rs}(\xi) = -\frac{1}{\beta^3 - 1} \left[\left(\frac{\beta}{\xi} \right)^3 - 1 \right] \quad (4.14)$$

$$S_{\varphi s}(\xi) = \frac{1}{2(\beta^3 - 1)} \left[2 + \left(\frac{\beta}{\xi} \right)^3 \right] \quad (4.15)$$

For comparison of the results, analogous relations obtained for the cylindrical casing (Włodarczyk *et al.*, 2005a) can be quoted:

— for the dynamic load

$$C_s = \frac{a^2 b^2}{b^2 - a^2} \frac{p}{2\mu} \quad \bar{C}_s = \frac{C}{a^2} = \frac{1}{2F} \frac{\beta^2}{\beta^2 - 1} \quad (4.16)$$

$$U(\xi, \eta) = \frac{1}{2F} \frac{\beta^2}{\beta^2 - 1} \frac{1}{\xi} (1 - \cos 2\pi\eta) = \frac{\bar{C}_s}{\xi} (1 - \cos 2\pi\eta) \quad (4.17)$$

$$V(\xi, \eta) = \frac{1}{F} \frac{\beta^2}{\beta^2 - 1} \sqrt{\frac{\beta^2 - 1}{2 \ln \beta}} \frac{1}{\xi} \sin 2\pi\eta \quad (4.18)$$

$$\varepsilon_{\varphi}(\xi, \eta) = -\varepsilon_r(\xi, \eta) = \frac{\bar{C}_s}{\xi^2} (1 - \cos 2\pi\eta) \quad (4.19)$$

$$S_r(\xi, \eta) = -\frac{1}{\beta^2 - 1} \left[\left(\frac{\beta}{\xi} \right)^2 - 1 \right] + A_r(\xi) \cos 2\pi\eta \quad (4.20)$$

$$A_r(\xi) = \frac{1}{\beta^2 - 1} \left[\left(\frac{\beta}{\xi} \right)^2 - 1 \right] - \frac{\ln(\beta/\xi)}{\ln \beta} \quad (4.21)$$

$$S_{\varphi}(\xi, \eta) = \frac{1}{\beta^2 - 1} \left[\left(\frac{\beta}{\xi} \right)^2 + 1 \right] - A_{\varphi}(\xi) \cos 2\pi\eta \quad (4.22)$$

$$A_{\varphi}(\xi) = \frac{1}{\beta^2 - 1} \left[\left(\frac{\beta}{\xi} \right)^2 + 1 \right] + \frac{\ln(\beta/\xi)}{\ln \beta} \quad (4.23)$$

$$\bar{\omega}_0 = \sqrt{\frac{2(\beta^2 - 1)}{\beta^2 \ln \beta}} \quad (4.24)$$

— for the static load

$$U_s(\xi) = \frac{1}{2F} \frac{\beta^2}{\beta^2 - 1} \frac{1}{\xi} = \frac{\overline{C}_s}{\xi} \quad (4.25)$$

$$\varepsilon_{\varphi s}(\xi) = -\varepsilon_{rs}(\xi) = \frac{\overline{C}_s}{\xi^2} \quad (4.26)$$

$$S_{rs}(\xi) = -\frac{1}{\beta^2 - 1} \left[\left(\frac{\beta}{\xi} \right)^2 - 1 \right] \quad (4.27)$$

$$S_{\varphi s}(\xi) = \frac{1}{\beta^2 - 1} \left[\left(\frac{\beta}{\xi} \right)^2 + 1 \right] \quad (4.28)$$

From the analysis of the relations presented above, it results that the considered casings loaded with the internal surge pressure $p = \text{const}$ respond like mechanical systems with one degree of freedom and vibrate radially with the angular frequency determined through formulae (4.11) and (4.24). The dynamic state of mechanical parameters of the loaded casings oscillates around their static values obtained for the statically generated pressure of the same value, i.e.: $p = p_s = \text{const}$.

The quantitative analysis of the mechanical parameters of studied casings is presented below.

5. Quantitative analysis of mechanical parameters of casings

We assume that the considered casings are made of steel which mechanical characteristics are: density in normal conditions $\rho_0 = 7800 \text{ kg/m}^3$, shear modulus $\mu = 75 \text{ GPa}$. The value of pressure has been set to $p = 400 \text{ MPa}$. For these values we have: $F = \mu/p = 187.5$, $c = \sqrt{\mu/\rho_0} = 3100 \text{ m/s}$. The remaining values of appropriate quantities are to be presented during analysis of particular parameters.

According to formulae (4.11) and (4.24), the relative angular frequencies of free vibration of the considered casings are functions of their walls thicknesses, which are characterized by the parameter β . Graphs of these functions are presented in Fig. 1.

It is seen that the angular frequencies decrease exponentially with the increase of wall thicknesses. This fact is caused by the increase of mass of the casings. It is significant that the angular frequency of the spherical casing is nearly twice greater than the angular frequency of a cylindrical one. It is caused

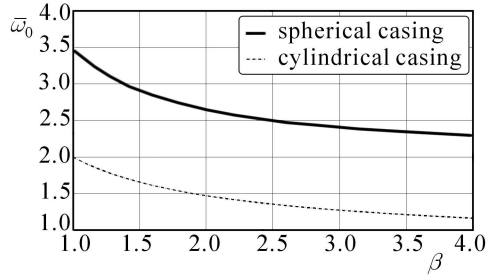


Fig. 1. Relative angular frequencies of free vibration of casings as functions of the parameter β

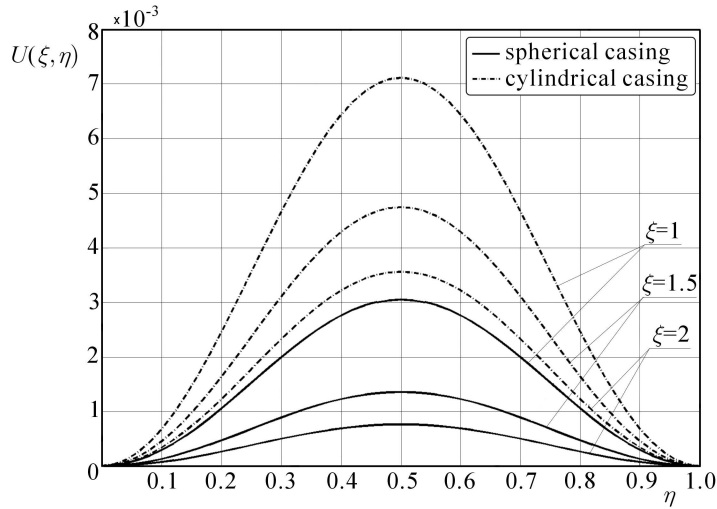


Fig. 2. Relative radial displacement of selected concentric surfaces of the casings within the range $0 \leq \eta \leq 1$ for selected values of the parameter ξ and $\beta = 2$

by greater stiffness of the spherical casing in comparison with the cylindrical casing of the same wall thickness.

The graphs of relative radial displacements of selected concentric surfaces of the casings are presented in Fig. 2. They are plotted according to formulae (4.4) and (4.17) for selected values of ξ and $\beta = 2$. The range $0 \leq \eta \leq 1$ contains the full free vibration period $0 \leq t \leq T_0$. It is significant that the radial displacement of the internal ($\xi = 1$) and remaining surfaces of casings has a positive value in the whole range. This means that during elastic vibrations forced with an internal pressure pulse, their internal diameters do not decrease below the initial values. The graphs depicted in Fig. 2 also show that the radial vibration amplitudes of particular concentric surfaces of spherical casings

are several times smaller than corresponding amplitudes of cylindrical casings. This indicates that the spherical casing is more rigid than the cylindrical one.

Like in the one-degree-of-freedom mechanical system, the dynamic coefficient of loading for both kinds of casings, according to formulae (4.4), (4.12), (4.17) and (4.25), is determined by the following expression

$$\Psi = \frac{U(\xi, \eta)}{U_s(\xi)} = 1 - \cos 2\pi\eta \tag{5.1}$$

and its maximum value is 2.

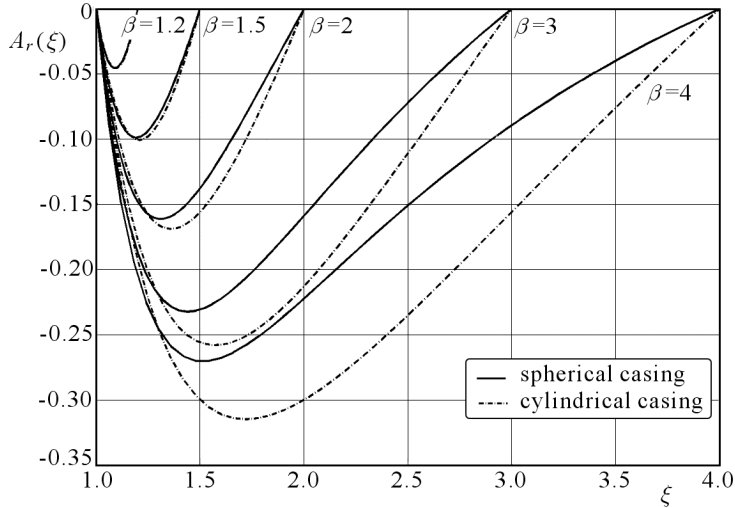


Fig. 3. Oscillation amplitudes $A_r(\xi)$ of relative radial stresses $S_r(\xi, \eta)$ in walls of the casings for selected values of their thickness ($\beta = 1.2, 1.5, 2, 3$ and 4)

In turn, the graphs of amplitudes $A_r(\xi)$ along the casing wall thickness ($1 \leq \xi \leq \beta$) for selected values of the parameter β are depicted in Fig. 3. It shows that the functions $A_r(\xi)$ have negative values in the whole range $1 \leq \xi \leq \beta$, and reach the minimum for $\xi = \xi_e$, where:

— for the spherical casing

$$\xi_e = \beta \sqrt{\frac{3}{\beta^2 + \beta + 1}} \tag{5.2}$$

— for the cylindrical casing

$$\xi_e = \beta \sqrt{2 \ln \frac{\beta}{\beta^2 - 1}} \tag{5.3}$$

Approaching the internal surfaces of casings ($\xi \rightarrow 1$), the amplitudes $A_r(\xi)$ decrease and reach zero for $\xi = 1$, according to the boundary condition ($S_r(1, \eta) \equiv -1$). The values of functions $A_r(\xi)$ for both kinds of casings are comparable for $\beta < 2$. For thicker walls, the differences between functions $A_r(\xi)$ for the cylindrical and spherical casing increase.

Analogous graphs of the oscillation amplitudes $A_\varphi(\xi)$ of the relative tangential stress S_φ in casing walls are presented in Fig. 4. The amplitudes $A_\varphi(\xi)$ are decreasing positive functions in the range $1 \leq \xi \leq \beta$. They reach their maxima at the internal surfaces of casings ($\xi = 1$), and the maximum values are determined by formulae:

— for the spherical casing

$$A_{\varphi_{max}} = \frac{3\beta^3}{2(\beta^3 - 1)} \quad (5.4)$$

— for the cylindrical casing

$$A_{\varphi_{max}} = \frac{2\beta^2}{\beta^2 - 1} \quad (5.5)$$

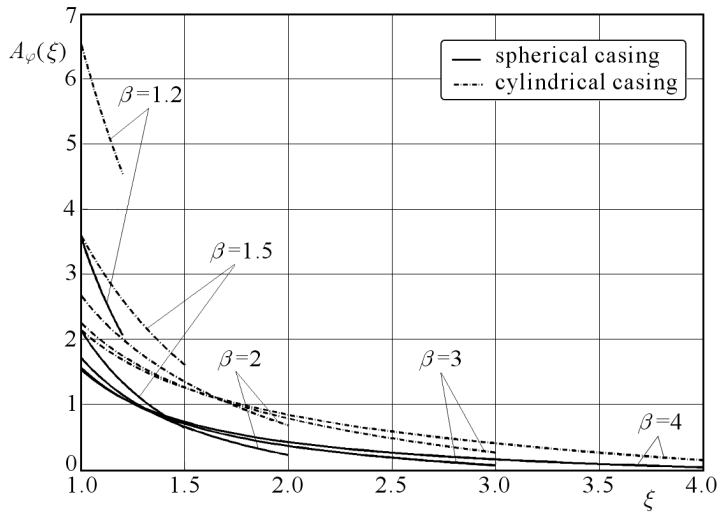


Fig. 4. Oscillation amplitudes of relative radial stresses $S_\varphi(\xi, \eta)$ in walls of the casings for selected values of their thickness ($\beta = 1.2, 1.5, 2, 3$ and 4)

From analysis of formulae (4.7), (4.8), (4.20) and (4.21), it results that the function $S_r(\xi, \eta)$ can change its sign from negative to positive (tension) on the inside casing wall. For $\eta = 0.5$ (the middle of the vibration period), this

happens in the spherical casing, when the parameter β characterizing the wall thickness satisfies the following inequality

$$\beta^4 + 2\beta^3 - 5\beta^2 - 6\beta + 5 > 0 \quad (5.6)$$

It is satisfied when $\beta > 1.79$. This means that in the wall of thickness characterized with $\beta = b/a < 1.79$, the radial tensile stress does not appear. The maximum positive value of the function $S_r(\xi, 0.5)$ for the spherical casing is reached on the surface determined as follows

$$\xi = \xi_e(\beta) = \beta \sqrt{\frac{6}{\beta^2 + \beta + 1}} \quad \beta > 1.79 \quad (5.7)$$

and amounts

$$S_{r_{max}}(\xi_e, 0.5) = \frac{1}{\beta - 1} \left(\frac{\beta}{\xi_e} - 1 \right) - \frac{2}{\beta^3 - 1} \left[\left(\frac{\beta}{\xi_e} \right)^2 - 1 \right] \quad (5.8)$$

Analogous relations for the cylindrical casing have the following form

$$\xi = \xi_e(\beta) = \exp\left(\frac{2(\beta^2 + 1) \ln \beta - \beta^2 + 1}{2(\beta^2 - 1)}\right) \quad \beta > 1.87 \quad (5.9)$$

$$S_{r_{max}}(\xi_e, 0.5) = \frac{\ln(\beta/\xi_e)}{\ln \beta} - \frac{2}{\beta^2 - 1} \left[\left(\frac{\beta}{\xi_e} \right)^2 - 1 \right]$$

Graphs of the function $S_r(\xi, \eta)$ are presented in Figs. 5-7.

The graphs presented in Fig. 5 for $\eta = 0.25$ correspond to the state of static load ($\cos 2\pi \cdot 0.25 = 0$). Values of the function $S_r(\xi, \eta)$ for $\eta = 0$ and $\eta = 0.5$ are symmetrically placed relative to the static plot. Graphs of the function $S_r(\xi, \eta)$ presented in Figs. 5 and 6 for both types of casings are qualitatively similar, but slightly differ quantitatively. Absolute values of the function $S_r(\xi, \eta)$ for the cylindrical casing are mostly greater than for the spherical one. This results from the fact that the displacement and strains for the same load and wall thickness are greater in the cylindrical casing (Fig. 2).

Analogous graphs of the function $S_\varphi(\xi, \eta)$ are presented in Figs. 8-10. It is significant that contrary to the function $S_r(\xi, \eta)$, the function $S_\varphi(\xi, \eta)$ changes its sign during vibrations for any value of the wall thickness. At the beginning

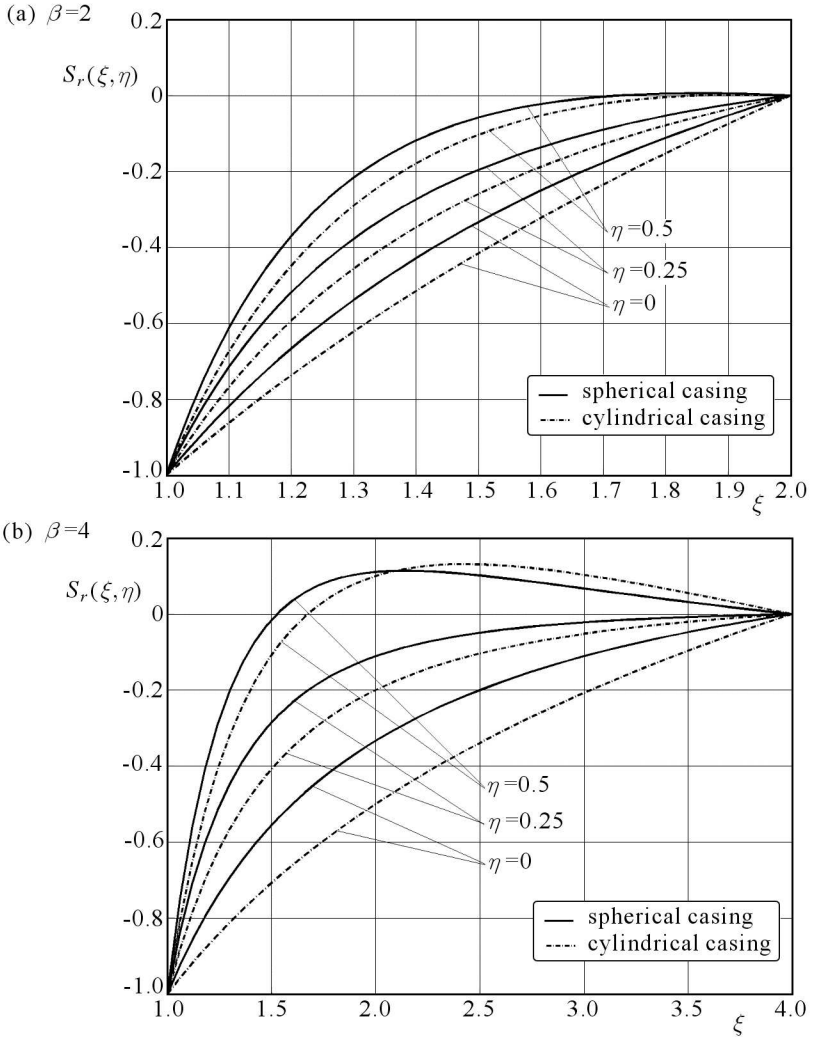


Fig. 5. Relative radial stress $S_r(\xi, \eta)$ as a function of the parameter ξ for $\eta = 0, 0.25$ and 0.5 and for $\beta = 2$ and $\beta = 4$

of the vibration period, the inertia of the casing wall causes a negative tangential stress (compression). Subsequently, the casing wall displaces radially and the sign of tangential stress changes to positive. The value of this stress reaches the maximum on the casing internal surface ($\xi = 1$) in the middle of the period ($\eta = 0.5$ – Fig. 8). The maximum values of the function $S_\varphi(\xi, \eta)$ for spherical and cylindrical casings are determined by the formulae:

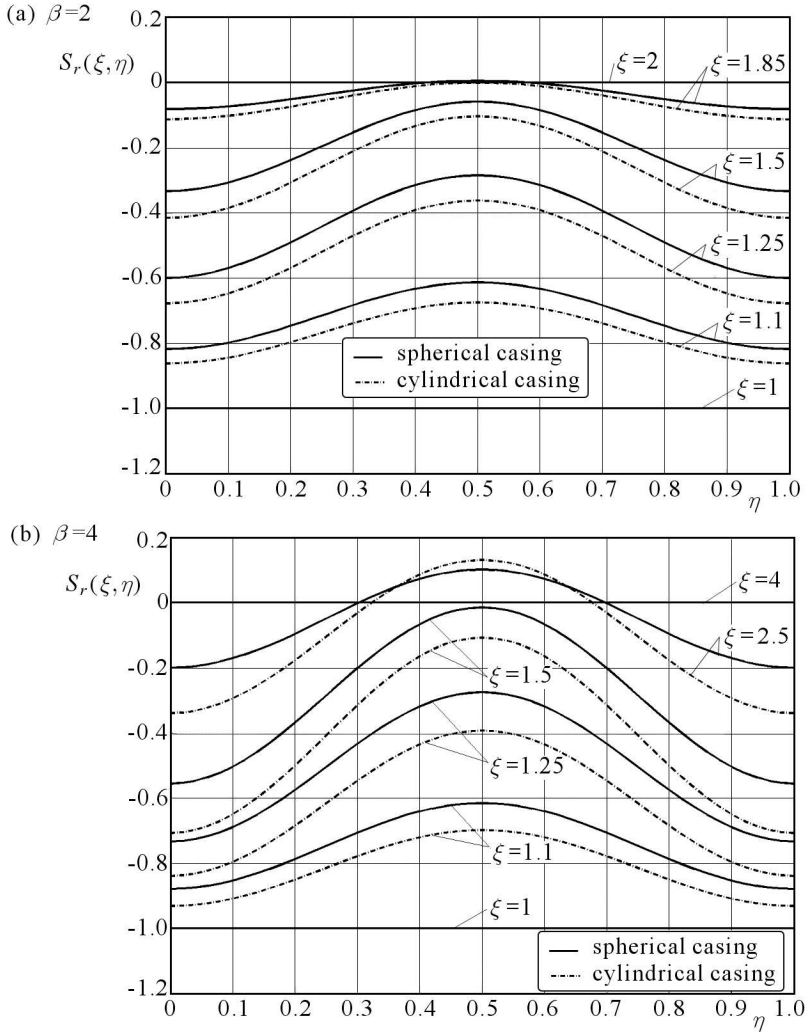


Fig. 6. Relative radial stress $S_r(\xi, \eta)$ as a function of the parameter η for selected concentric surfaces of the wall and for $\beta = 2$ and $\beta = 4$

— for the spherical casing

$$S_{\varphi_{max}} = \frac{2\beta^3 + 1}{\beta^3 - 1} \quad (5.10)$$

— for the cylindrical casing

$$S_{\varphi_{max}} = \frac{3\beta^2 + 1}{\beta^2 - 1} \quad (5.11)$$

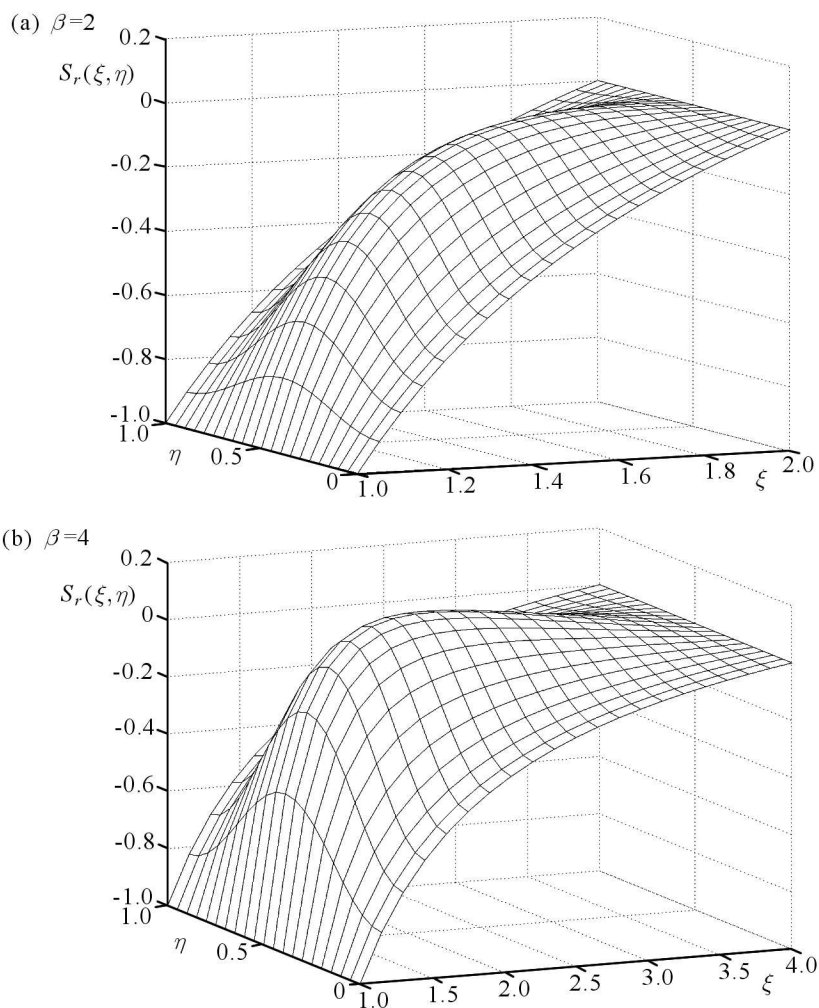


Fig. 7. Spatial graph of the function $S_r(\xi, \eta)$ for the spherical casing

From the analysis of graphs presented in Figs. 8-10, it results that, like in the case of the function $S_r(\xi, \eta)$, plots of the function $S_\varphi(\xi, \eta)$ for spherical and for cylindrical casings are qualitatively similar, but the quantitative differences are significant. It is seen that for the same diameters, wall thicknesses and internal pressure pulses, the tangential stress is greater in the cylindrical casing.

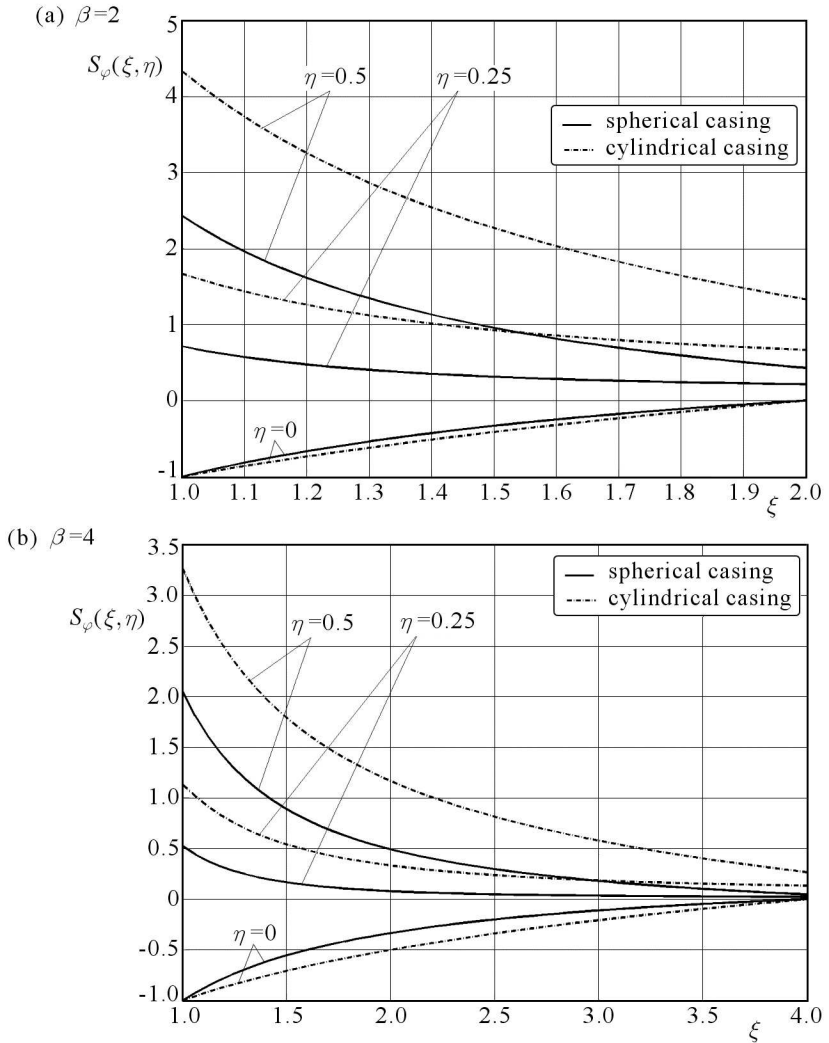


Fig. 8. Relative tangential stress $S_\varphi(\xi, \eta)$ as a function of the parameter ξ for $\eta = 0, 0.25$ and 0.5 and for $\beta = 2$ and $\beta = 4$

6. Final conclusions

From the analysis of the considered problem, the following conclusions can be drawn:

- Thick-walled casings with cylindrical or spherical symmetry loaded with an internal pressure pulse vibrate radially with an angular frequency ω_0 and behave like one-degree-of-freedom systems. For equal diameters and

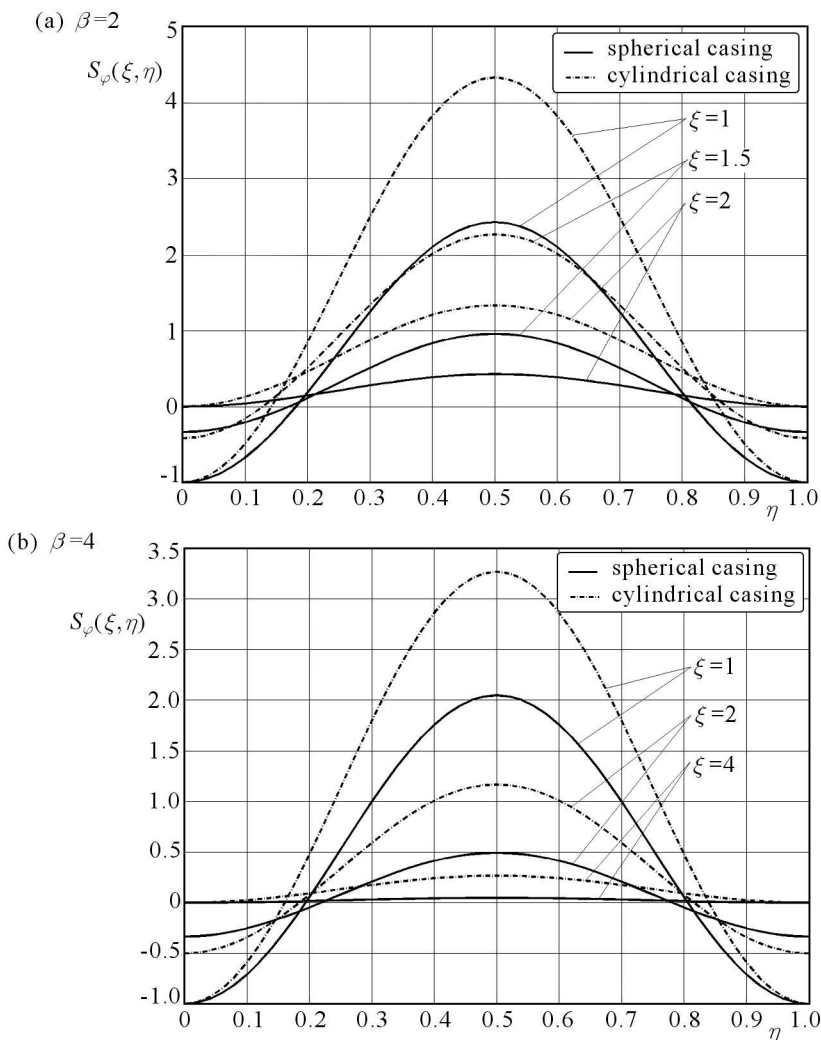


Fig. 9. Relative tangential stress $S_\varphi(\xi, \eta)$ as a function of the parameter η for selected concentric surfaces of the wall and for $\beta = 2$ and $\beta = 4$

wall thicknesses, the pulsance of free vibrations of the spherical casing is nearly twice greater than that in the cylindrical one. It is caused by greater stiffness of the spherical casing.

- The maximum value of the dynamic coefficient of loading is $\Psi = 2$.
- From the analytical solution to the problem, it directly results that the dynamic states of radial displacement u , strains ε_r , ε_φ and stresses σ_r , σ_φ generated in the casing walls by the internal pressure $p(t)$

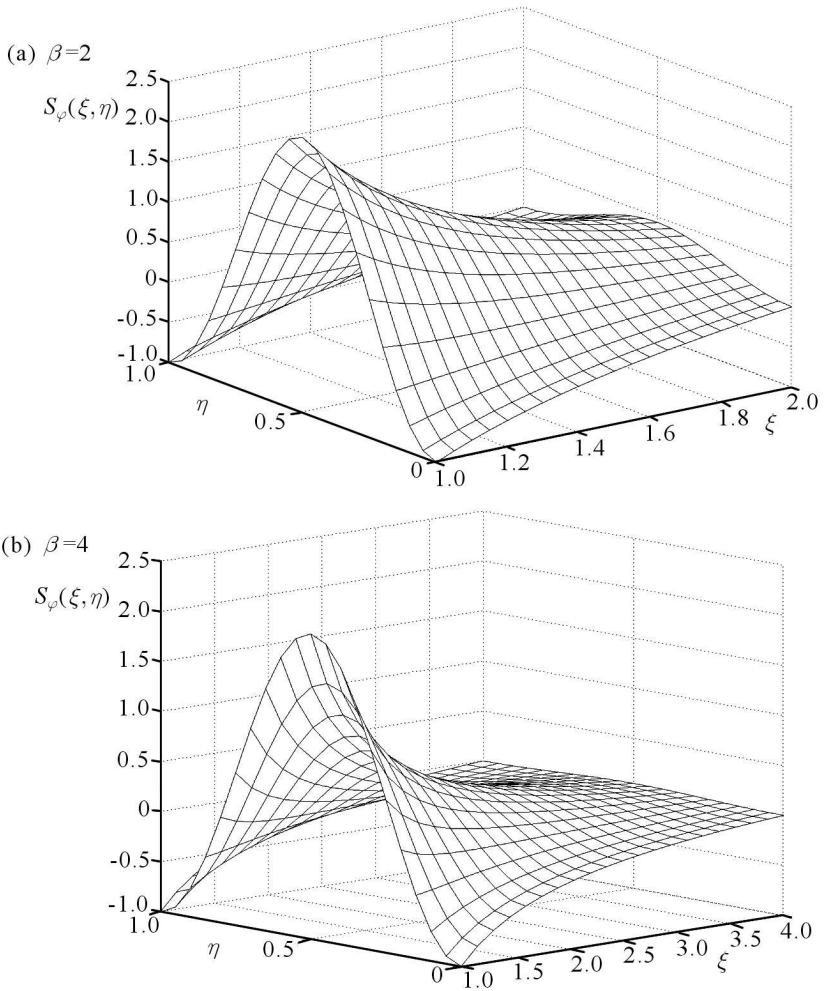


Fig. 10. Spatial graphs of the function $S_\varphi(\xi, \eta)$ for the spherical casing

are determined through their material physical properties ρ_0 , μ , casings geometry a , b and the character of changes of the pressure described by a time function $p(t)$.

References

1. DŻYGADŁO Z., KALISKI S., SOLARZ L., WŁODARCZYK E., 1966, *Vibration and Waves in Solids* [in Polish], Warszawa, PWN

2. NOWACKI W., 1970, *Theory of Elasticity* [in Polish], Warszawa, PWN
3. WALTERS W.P., ZUKAS J.A., 1989, *Fundamentals of Shaped Charges*, New York: A. Wiley – Interscience Publication
4. WŁODARCZYK E., JANISZEWSKI J., 2004, Static and dynamic ductility of copper and its sinters, *J. Tech. Phys.*, **45**, 4, 263-274
5. WŁODARCZYK E., JANISZEWSKI J., MAGIER M., 2004, Analysis of axial stress concentration in core of elongated sabot shell during fire [in Polish], *Biul. WAT*, **LIII**, 2/3, 109-132
6. WŁODARCZYK E., GŁODOWSKI Z., PASZKOWSKI R., 2005a, A thick-walled pipe radial vibrations forced by pulsed internal pressure [in Polish], *Biul. WAT*, **LIV**, 10, 31-48
7. WŁODARCZYK E., JANISZEWSKI J., GŁODOWSKI Z., 2005b, Dynamical state of stress and strain in thin-walled explosively expanded metal ring [in Polish], *Biul. WAT*, **LIV**, 2/3, 109-119

Dynamika grubościennej kulistej osłony obciążonej wewnętrznym ciśnieniem zmiennym w czasie

Streszczenie

Zbadano problem radialnych drgań grubościennej osłony kulistej obciążonej udarowo wewnętrznym ciśnieniem impulsowym. Założono, że materiał osłony jest sprężyste nieściśliwy. Przy takim uproszczeniu uzyskano zamknięte analityczne rozwiązanie zagadnienia dynamiki osłony kulistej w ramach liniowej teorii sprężystości. Okazuje się, że osłona kulista wykonana z materiału nieściśliwego, podobnie jak rura, obciążona wewnątrz udarowo, zachowuje się jak układ o jednym stopniu swobody. Częstotliwość kołowa drgań własnych osłony kulistej jest kilkakrotnie większa od częstotliwości rury o tej samej średnicy wewnętrznej i grubości ścianki. Przedstawione rozwiązanie można wykorzystać do szacowania wytrzymałości kulistych osłon balistycznych stosowanych przy wybuchowym napędzaniu cienkościennych pierścieni używanych w badaniach dynamicznych właściwości materiałów. Poza tym, przedstawione wyniki badań dają dodatkowy wkład wiedzy do teorii drgań technicznych układów ciągłych.

Manuscript received March 9, 2007; accepted for print October 3, 2007